Extracellular matrix formation in self-assembled minimalistic bioactive hydrogels based on aromatic peptide amphiphiles

Mi Zhou[1], Rein V Ulijn[2] and Julie E Gough[1]

Abstract

The hitherto inconsistency in clinical performance for engineered skin drives the current development of novel cell-scaffolding materials; one challenge is to only extract essential characteristics from the complex native ECM (extracellular matrix) and incorporate them into a scaffold with minimal complexity to support normal cell functions. This study involved small-molecule-based bioactive hydrogels produced by the co-assembly of two aromatic peptide amphiphiles: Fmoc-FF (Fluorenylmethoxycarbonyl-diphenylalanine) and Fmoc-RGD (arginine–glycine–aspartic acid). Three-dimensionally cultured human dermal fibroblasts deposited dense ECM networks including fibronectin and collagen I within the hydrogels in a 14-day culture. The fibroblasts organized the fibrous ECM and contracted the gel without differentiating into myofibroblasts. The stiffness of the cell-gel constructs increased dramatically due to ECM formation and gel contraction. This created an economical biomimetic model-scaffold to further understand skin reconstruction *in vitro* and supplied a design pathway to create versatile cell-scaffolds with varied bioactivities and simplicity.

Introduction

Dermal fibroblasts have a main function *in vivo* to synthesize and secrete extracellular matrix, and to organize and remodel it extracellularly.[1] The ECM of dermis is abundant and three-dimensional (3D), so its main component such as collagen carries the major mechanical loads for the cells; it is also complex and contains a plethora of proteins, proteoglycans and polysaccharides to support native cells for their adhesion, growth, division and differentiation through cell-matrix interactions.[2] To engineer a dermal tissue equivalent, an *in vitro* 3D cell-matrix should physically support cell survival and biologically guide the cells towards regenerating their own ECM. Various 3D cell-scaffolds have been developed in skin reconstruction with natural[3,4] or synthetic[5–7] polymers or their mixtures[8,9] included and various biological cues incorporated through introducing biopolymers.[10,11] Although these natural/synthetic polymeric hybrid scaffolds have been produced to precisely control mechanical characteristics of initial scaffolds as well as hydrogel degradation patterns, short biofunctional moieties extracted from large biopolymers (e.g. proteins) provided more tailorable alternatives for enhancing bioavailability and bioactivity compared to large biopolymers.[12] These short biological moieties have been linked onto synthetic polymers through chemical bonds,[13–15] and these modified polymers were then made into 3D bioactive scaffolds. Instead of polymers, small molecules were designed which could self-assemble into supra-molecules and macroscopically form 3D-hydrogel scaffolds,[16–24] and short biological cues were grafted onto the small molecules/self-assembling moieties. This approach allowed precise design down to the molecular

[1]School of Materials, University of Manchester, Manchester, UK
[2]Department of Pure and Applied Chemistry, University of Strathclyde, Glasgow, UK

Corresponding author:
Julie E Gough, The University of Manchester, Grosvenor Street, Manchester, M13 9PL, UK.
Email: j.gough@manchester.ac.uk

level to tailor biological cue position, conformation and density, and these systems have been attempted to interact with cells with the aim of engineering varied tissues *in vitro* .[16,17,20,21,23,24] The RGD ligands known to promote cell adhesion have been the simplest molecular candidate incorporated into both the polymeric systems[14,15] and the small-molecule-based systems.[16,17,20,22,24] Different cell types were cultured within these scaffolds with different aims within the regenerative medicine field (e.g., cell differentiation,[16] cell growth[20,24]), and other motifs alongside RGDs were usually used simultaneously to generate a certain cell response[16,17,20,24] including ECM formation.[17]

We have previously designed a novel biomimetic nanofibrous hydrogel based on co-assembly of a structural (Fmoc-FF) and a functional (Fmoc-RGD) building block, which was shown to have the ability to support attachment, spreading and proliferation of encapsulated human dermal fibroblasts.[25] The novelty of this hydrogel resides in its simple yet bioactive structure in comparison to other studies using much longer and therefore expensive peptide sequences. Also, due to its versatility, it can be functionalized with other bioactive ligands, furthering the system's applications. Cell spreading was initiated via interaction of cell $\alpha5\beta1$ integrins with RGD ligands within the hydrogels. It remained a question whether this single biological motif (RGDs) incorporated into the small-molecule-based hydrogel could elicit further *in vitro* dermal reconstruction without the addition of other motifs or growth factors. Therefore, the ability of the bioactive scaffold to further encourage fibroblast secretion and organization of ECM and to reconstruct a normal dermal tissue analogue with enhanced mechanical strength is the focus of this study.

Materials and methods

Two-dimensional-expansion of primary human dermal fibroblasts

Primary dermal fibroblasts from a human adult (HDFa; Cascade Biologics Inc., UK) were expanded on tissue culture plastic (TCP) in HDFa growth medium (Dulbecco's modified Eagle's medium (DMEM) supplemented with 10% v/v foetal bovine serum (FBS) and 1% v/v antibiotic–antimycotic solution). Subcultures of the cells were performed using a 0.05% m/v trypsin-EDTA (0.53 mM) solution for 5 min at 37°C when the cultures reached 70%–80% confluence. All the reagents for cell expansions were supplied by Gibco®, Life Technologies Ltd, UK.

Cell encapsulation within the peptide-based hydrogels

Aqueous solutions of Fmoc-peptides were prepared as previously reported.[1] To prepare a 20-mM Fmoc-FF solution,

2 mL distilled water (dH_2O, Gibco) and 100 µL of 0.5 M sodium hydroxide (NaOH; Fisher Scientifics Ltd, UK) were pipetted into a 10-mL glass vial which contained 0.0214 g of Fmoc-FF (Bachem GmbH, Germany). Alternate vortex and ultra-sonication were applied until a clear solution was obtained. To prepare a 20-mM Fmoc-RGD solution at pH 3, 2 mL dH_2O and 80 µL of 0.5 M hydrochloric acid (HCl; Sigma-Aldrich Co. Ltd, UK) was added into a glass vial with 0.0228 g of Fmoc-RGD (Synthetech Inc., USA). Continuous ultra-sonication was applied until a transparent solution was formed. Similarly, 20-mM Fmoc-RGE solution was prepared by dissolving 0.0232 g of the peptide (Synthetech Inc., USA) into 2 mL dH_2O containing 80 µL of 0.5 M HCl. The mixed Fmoc-FF/RGD or Fmoc-FF/RGE solutions were then prepared by mixing 1.4 mL 20-mM Fmoc-FF at pH 10.0 with 0.6 mL 20-mM Fmoc-RGD (or Fmoc-RGE) at pH 3; 98 µL 0.5 M NaOH (or 24 µL for Fmoc-FF/RGE) was added to ensure homogeneity. The mixed solutions were further neutralized to pH 7.0 with drop-wise addition of 0.5 M HCl. Prior to their dissolution, a 30-min UV sterilization was applied to the Fmoc-peptide powders.

For cell encapsulation, the prepared Fmoc-peptide solutions were warmed to 37°C. Passage 5 HDFa were trypsinized and re-suspended into DMEM (without FBS) to a density of 10^7 cell/mL; 100 µL of either Fmoc-peptide solution was placed into a tissue culture insert (Greiner Bio One Ltd, UK) in a well of a 12-well plate, and an equal volume of cell suspension was added. An immediate yet gentle shaking was applied to ensure homogeneity; 2 mL of HDFa growth medium was then pipetted into the well containing the insert, and the culture was maintained in a 37°C/5% CO_2 incubator for gelation. After 30 min, an extra 200 µL of growth medium was placed on top of each cell-gel construct. The medium surrounding the inserts and on top of the constructs was changed 2 h post culture and then daily.

Immunofluorescence

Deposited ECM in the cell-gel constructs

At 1, 3, 7 and 14 days post culture, the cell-gel constructs were fixed with 4% m/v paraformaldehyde in phosphate buffered saline (PBS, Gibco) for 30 min and then permeablized with 0.5% v/v Triton-X100 in PBS for 5 min at 4°C. Prior to immuno-staining, the samples were blocked in 1% m/v bovine serum albumin (BSA) in PBS for 6 h with the blocking solution changed every 2 h.

For fibronectin detection, the samples were incubated overnight with a primary antibody (p-ab) of rabbit anti-human fibronectin (dilution factor: 1:100) at 4°C. This was followed by a 4-h soak in 1% m/v BSA in PBS, and the BSA solution was replaced hourly. After the removal of the p-ab, a secondary antibody (s-ab) of Cy3-conjugated

sheep anti-rabbit IgG (dilution factor: 1:100) was used to incubate with the samples for 6 h. To remove the s-ab, a 4-h wash with 1% BSA in PBS was given to the samples with the BSA solution changed hourly. The samples were then mounted with Prolong® gold anti-fade reagent with DAPI (Life Technologies Ltd, UK) and cured for 24 h before sealing with nail varnish. A Nikon Eclipse 50i fluorescence microscope with excitation filters of 547 nm (Cy3) and 340 nm (DAPI) was used to observe the immunofluorescence.

The immuno-staining of collagen I and III followed the same procedure used for the FN staining. A primary rabbit anti-human collagen I antibody (dilution factor: 1:40) and a primary mouse anti-human collagen III antibody were used respectively to detect collagen I and III. The s-abs of Cy3-conjugated sheep anti-rabbit IgG (dilution factor: 1:100) and FITC-conjugated rabbit anti-mouse IgG (Life Technologies Ltd, UK; dilution factor: 1:100) were used separately to bind the p-abs. The immunofluorescence was observed by the Nikon Eclipse 50i fluorescence microscope with excitation filters of 547 nm (Cy3), 495 nm (FITC) and 340 nm (DAPI).

Alpha-smooth muscle actin

Alpha (α)-smooth muscle actin within the cytoskeleton was also examined following the same immuno-staining procedure. A p-ab of rabbit anti-human α-smooth muscle actin (dilution factor: 1:50) and an s-ab of Cy3-conjugated sheep anti-rabbit lgG (dilution factor: 1:100) were used for binding to the actins. The p-abs for all above immuno-stainings were provided by Abcam plc, UK, and other reagents were supplied by Sigma-Aldrich Co. Ltd, UK, unless stated separately.

Rheology of cell-containing peptide-based hydrogels

Visco-elastic characteristics of the cell-containing hydrogels were measured using a Bohlin C-VOR rheometer in an oscillatory mode. Each 200-μL cell-gel construct was placed between a 20-mm/2° cone plate and a flat stationary plate; the gap between the two plates was 70 μm for the 1-h samples and 20 μm for the 7-day samples. A solvent trap was used to keep the sample hydrated, and an integrated temperature controller was used to maintain the temperature of the sample stage at 25°C. A combined measurement including an 'amplitude sweep' and a 'frequency sweep' was performed on each sample. The 'amplitude sweep' was performed by applying controlled stresses that were linearly increased from 0.5 to 100 Pa and strains corresponding to the stresses were recorded; the oscillatory frequency was maintained at 1 Hz. The maximum strain within the linear visco-elastic region was chosen from the 'amplitude sweep' for the 'frequency sweep', in which the

stress is altered to obtain the chosen strain, and elastic and viscous moduli were measured as a function of frequency between 1 and 100 Hz. Log G' or Log G'' was plotted against frequency to obtain a rheological spectrum.

Results

Deposition of ECM and fibroblast phenotype in the cell-containing hydrogels

Presence of fibronectin, collagen III and collagen I, the essential dermal ECM components secreted sequentially in wound healing, was examined in the 3D HDFa-containing Fmoc-FF/RGD (molar ratio: 7:3 for Fmoc-FF:Fmoc-RGD or RGE, at a 20 mM total concentration) hydrogels.

Within the 14-day culture, fibronectin secretion and its organization into a dense fibrous mesh was observed in the cell-containing Fmoc-FF/RGD hydrogels (Figure 1(a)–(d)). Its counterpart Fmoc-FF/RGE hydrogel, however, only had cells surrounded by red structureless staining (only in close proximity to the cells) through the 14-day culture (Figure 1(e)–(h)). As shown in Figure 2(a) and (e), at day 1, only structureless red staining around the cell periphery was observed for both Fmoc-FF/RGD and Fmoc-FF/RGE cell-gel constructs. An obvious increase of secreted FN was noticed at day 3 for the RGD-containing gel evidenced by an increased intensity of the red staining and certain visible fibrous structures (Figure 1(b)). Between day 3 and day 14, FN continued to deposit in the cell-containing Fmoc-FF/RGD hydrogels (Figure 1(c)–(d)) and a dense filamentous network of FN was deposited within the 3D cell-gel constructs at day 14 (Figure 1(d)).

Collagen I, a major protein laid down within dermal wounds by fibroblasts, was observed to deposit inside the cell-containing Fmoc-FF/RGD hydrogels along with FN, and it also formed dense fibrous networks (Figure 2(a)–(d)). This protein appeared later than FN in the RGD gel, as on day 1 and 3 lesser cells had collagen staining around their periphery (Figures 1(a) and (b) and 2(a) and (b)) and staining intensity was lower. From day 3, loosely scattered fine collagen fibres became visible (Figure 2(b)), and at day 14, the collagen mesh appeared denser than that of the FN network (Figures 1(d) and 2(d)). In the Fmoc-FF/RGE, collagen I was also observed but later than in the RGD gels (Figure 2(e)–(h)), as on day 1, there was little visible collagen deposition (Figure 2(e)). The major appearance of collagen I in the RGE gels was structureless, with staining around cell peripheries observed although the amount of staining increased with time (Figure 2(f)–(h)). By day 14, the density and intensity of the red staining was lower compared to that in the RGD counterparts and fibrous network was less visible (Figure 2(d) and (h)).
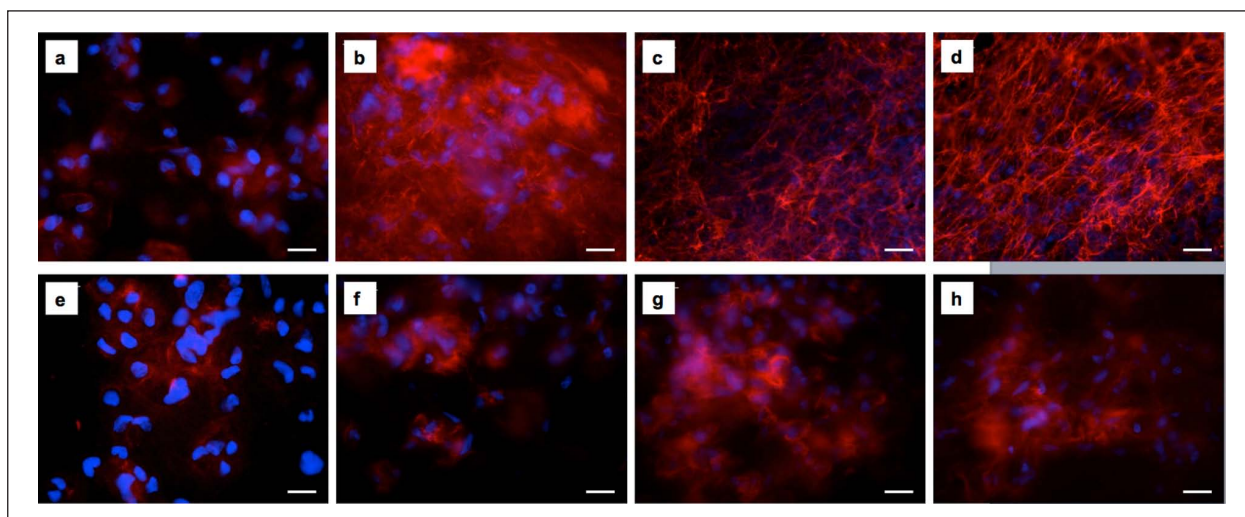
Figure 1. Fluorescence micrographs of fibronectin secretion by HDFa cells 1, 3, 7 and 14 days post culture within Fmoc-FF/RGD and Fmoc-FF/RGE hydrogels. Fibronectin deposited and eventually formed a filamentous network in the Fmoc-FF/RGD hydrogel (a) 1, (b) 3, (c) 7 and (d) 14 days post culture. Fibronectin was much less expressed in the Fmoc-RGE gel with structureless staining observed (e) 1, (f) 3, (g) 7 and (h) 14 days post culture. Blue: cell nuclei; Red: fibronectin. Scale bars: 25 μm.
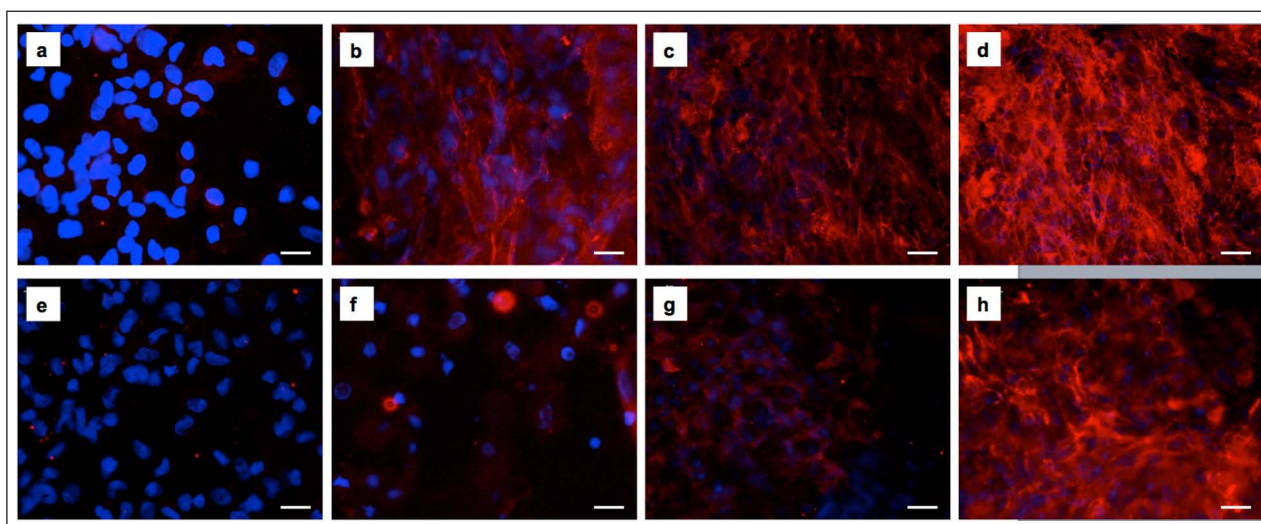

Figure 2. Fluorescence micrographs of collagen I secretion by HDFa cells 1, 3, 7 and 14 days post culture within Fmoc-FF/RGD and Fmoc-FF/RGE hydrogels. Collagen I was deposited and organized into a dense fibrous network in the Fmoc-FF/RGD hydrogel through the culture term (a) 1, (b) 3, (c) 7 and (d) 14 days post culture. Collagen I was much less expressed in the Fmoc-RGE gel with structureless staining observed (e) 1, (f) 3, (g) 7 and (h) 14 days post culture. Blue: cell nuclei; Red: collagen I. Scale bars: 25 μm.

Collagen III, also secreted in wound healing, was not detected in either cell-containing substrates during the 14-day culture (Figure 3(a)). In the Fmoc-FF/RGD gel, the dermal fibroblast had an elongated spindle-like morphology resembling myofibroblasts, especially for cells around the periphery of the hydrogel during the gel contraction period.[25] However, alpha-smooth muscle actin, a marker for fibroblast differentiation into myofibroblasts in collagen gel contraction models, was also not observed within these cells through the gel contraction (Figure 3(b)).

Visco-elasticity of cell-containing hydrogels

One hour after mixing HDFa cells into the Fmoc-FF/RGD solution, the viscous moduli (G'') of the cell-containing mixtures became lower than their elastic moduli (G'); this was shown in the oscillating rheological spectrum (Figure 4(a)) collected with a fixed strain. The G'' was 2.9–4.2 times lower than G' with phase angles between 13.4° and 18.6°. The characteristics of a lower G'' compared to G' and a small phase angle both

indicated that the mixtures already became solids, and this information was supported by their appearances at 1 h post culture as self-supporting hydrogels (previously reported[25]). At 1 h, the average G′ for the cell-containing Fmoc-FF/RGD was 786.3 Pa, and the data showed the G′ at 1 h was significantly lower ($p < 0.05$) than that of the Fmoc-peptide hydrogels without cells (previously reported[25]). The lower G′ for these cell-containing mixtures, as a representative of lower material stiffness, suggested that the encapsulated cells might interfere with the gelation.

The cell-containing Fmoc-FF/RGD gels underwent further molecular assembly through the culture period, while they also underwent cell-assisted contractions (previously reported[25]). Both processes increased the stiffness of the mixtures; as observed (Figure 4(b)), the average G′ of the 7-day Fmoc-FF/RGD increased to 7234 Pa through the 7-day culture, which was nearly a magnitude higher (9.2 fold) than that of their 1-h counterparts. Sample variations were noticed especially for the 1-h samples as the standard errors for G′ (standard deviation/average G′) among samples was 47.6%.
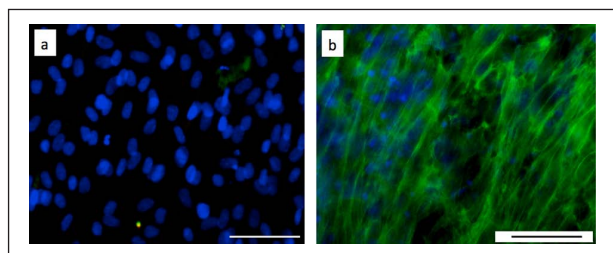

Figure 3. (a) Collagen III formation in the HDFa-containing Fmoc-FF/RGD hydrogel was not observed 14 days post culture (blue: cell nuclei; green: collagen III). (b) Elongated HDFa cells in the Fmoc-FF/RGD hydrogel 7 days post culture showed no expression of α-smooth muscle actin (blue: cell nuclei; green: F-actins; red: α-smooth muscle actins). Scale bars: 50 µm.

The differences among samples were a result of the manual process in cell encapsulation. The sample variation was seen to drop at the end of the culture to 29.3%.

Discussion

Alongside cell proliferation and hydrogel contraction (previously reported[25]), deposition of significant native dermal ECM components and increased stiffness were another two novel and important characteristics detected in this study for the cell-containing Fmoc-FF/RGD hydrogels. Few hydrogel systems can claim long-term culture and extensive ECM formation leading to improved mechanical properties. FN, collagen I and III are known to be secreted at different stages of the wound healing process, and each possesses unique responsibilities for the regeneration of the dermis. Through the 14-day culture, both fibronectin and collagen I were observed within the Fmoc-FF/RGD hydrogels; their deposition appeared as dense interwoven fibre networks by day 14. The Fmoc-FF/RGE hydrogel had much less amounts of these two proteins secreted, and at the end of the culture, filamentous protein networks were not noticeable. This suggested that cell adhesion through specific RGD-integrin binding not only supported cell spreading and proliferation (previously reported[25]), but also encouraged cell secretion of fibronectin and collagen I and supported 3D-organization of these native ECM components outside the cells.

For the Fmoc-FF/RGD gels, it was also observed that FN was deposited ahead of collagen I, which also occurs in natural wound healing.[26,27] As a glycoprotein with multi-adhesive sites for binding to both ECM and cells,[28] the initial secreted FN could provide a substrate for both cell movement and collagen I deposition within the 3D-matrix. As collagen I is the dominant collagen in normal dermis, the later presence of a denser collagen I network in the RGD gels indicated *in vitro* formation of a normal dermal tissue within the scaffold. However, the *in vitro* dermal
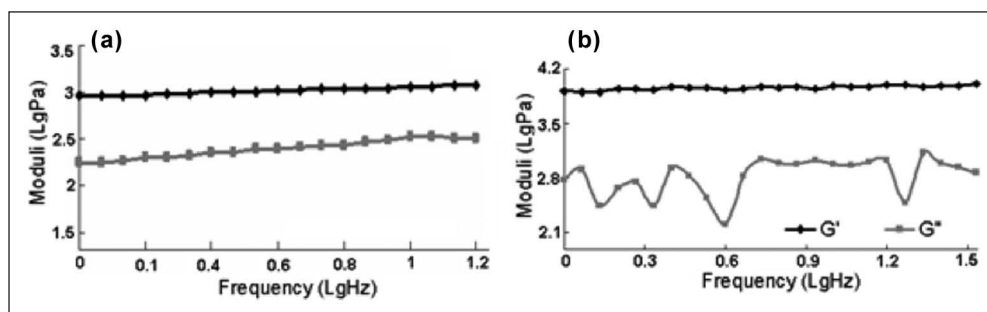

Figure 4. Visco-elasticity of the cell-containing Fmoc-FF/RGD hydrogels 1 h and 7 days post culture. (a) Rheological charts showing elastic moduli (G′) and viscous moduli (G″) in a frequency sweep for the cell-containing Fmoc-FF/RGD mixtures 1 h post culture. (b) A rheological chart showing elastic moduli (G′) and viscous moduli (G″) in a frequency sweep for the cell-containing Fmoc-FF/RGD mixtures 7 days post culture.

reconstruction did not fully mimic *in vivo* wound regeneration; collagen III, the collagen first deposited in wounds and later replaced by collagen I,[29] was not observed on/in any of the substrates. This could be due to absence of complex biological factors (e.g., cytokines) presented at *in vivo* wound sites.

Beside ECM secretion, the HDFa cells also actively contracted the RGD-containing gels as previously reported.[25] They adopted an elongated morphology and aligned especially along the gel circumferences (Figure 3(b)). However, no differentiation into myofibroblasts was detected as alpha-smooth muscle actin was not observed, and gel contraction was, therefore, by normal fibroblasts pulling and organizing the nanofibrous 3D-networks.

The visco-elasticity shown by the rheological data suggested that 1 h post cell encapsulation, the cell-containing hydrogels became self-supporting with G' higher than G''. Their G', however, was lower at 1 h compared to their counterparts without cells. The incorporated cells acted as micro-scaled particles dispersed within the system; they affected homogeneity of the self-assembling system as suggested also by the high standard errors among 1-h samples, and therefore slowed molecular assembly and growth of the self-assembled nanofibres. Despite the inference from the cells, the self-assembled fibrous networks formed on time to provide the cells with a supportive 3D-matrix for initial cell attachment.

Seven-day cell-containing Fmoc-FF/RGD hydrogels possessed much higher stiffness compared to their day-1 counterparts (9.2 fold higher than the latter), and also to the 7-day RGD gels without cells (previously reported[25]). This suggested that ECM formed inside the cell-containing Fmoc-FF/RGD hydrogels to strengthen the self-assembled fibrous networks, and this was confirmed by the observed presence of dense fibronectin and collagen I meshes in the gels. As reported,[1] gel contraction also occurred in the RGD-containing gels when cells were present; this could further concentrate the inner fibrous structures and raise the hydrogel stiffness.

Conclusion

Dermal fibroblasts secreted a large amount of ECM within these simple Fmoc-FF/RGD scaffolds which formed dense fibrous networks. The deposited ECM together with cell-assisted gel contraction provided the cell-gel constructs with high stiffness, and the gel contraction was through normal fibroblasts without their differentiation into myofibroblasts. RGDs in this self-assembling system induced the *in vitro* dermal regeneration as without the tri-peptides, normal functions of fibroblasts including spreading, proliferation, ECM secretion and organization were not observed. A diversity of peptide sequences with various bio-functions and other amino-acid residues able to stabilize or strengthen the hydrogel structure may be recruited through the same molecular self-assembly approach. This may fulfil other requirements in skin engineering including angiogenesis, and may also provide varied 3D tissue models to study in the cell-therapy and tissue engineering areas.

References

1. Wenstrup RJ, Murad S and Pinnell SR. Collagen. In: Goldsmith LA (ed.) *Physiology, biochemistry, and molecular biology of the skin*. New York; Oxford: Oxford University Press, 1991, pp. 481–509.
2. Alberts B, Bray D, Hopkin K, et al. Tissues and cancer. In: Alberts B, Bray D, Hopkin K, et al. (eds) *Essential cell biology*. New York; London: Garland Science Press, 2004, pp. 698–706.
3. Bell E, Ehrlich HP and Buttle DJ. Living tissue formed in vitro and accepted as skin-equivalent tissue of full thickness. *Science* 1981; 211: 1052–1054.
4. Gentzkow GD, Iwasaki SD, Hershon KS, et al. Use of dermagraft, a cultured human dermis, to treat diabetic foot ulcers. *Diabetes Care* 1996; 19: 350–354.
5. Ng KW, Khor HL and Hutmacher DW. In vitro characterization of natural and synthetic dermal matrices cultured with human dermal fibroblasts. *Biomaterials* 2004; 25: 2807–2818.
6. Lee C, Kung P and Lee Y. Preparation of poly (vinyl alcohol)-chondroitin sulphate hydrogel as matrices in tissue engineering. *Carbohyd Polym* 2005; 61: 348–354.
7. Ghalbzouri AE, Lamme EN, van Blitterswijk C, et al. The use of PEGT/PBT as a dermal scaffold for skin tissue engineering. *Biomaterials* 2004; 25: 2987–2996.
8. Ng KW, Louis J, Ho BST, et al. Characterization of a novel bioactive poly[(lactic acid)-co-(glycolic acid)] and collagen hybrid matrix for dermal regeneration. *Polym Int* 2005; 54: 1449–1457.
9. Venugopal JR, Zhang Y and Ramakrishna S. In vitro culture of human dermal fibroblasts on electrospun polycaprolactone collagen nanofibrous membrane. *Artif Organs* 2006; 30(6): 440–446.
10. Wang T, Wu H, Huang Y, et al. Biomimetic bilayered gelatin-chondroitin 6 sulphate-hyaluronic acid biopolymer as a scaffold for skin equivalent tissue engineering. *Artif Organs* 2006; 30(3): 141–149.
11. Tibbitt MW and Anseth KS. Hydrogels as extracellular matrix mimics for 3D cell culture. *Biotechnol Bioeng* 2009; 103: 655–663.
12. Lau TT and Wang D. Bioresponsive hydrogel scaffolding systems for 3D constructions in tissue engineering and regenerative medicine. *Nanomedicine* 2013; 8(4): 655–668.

13. Hubbell JA. Bioactive biomaterials. *Curr Opin Biotechnol* 1999; 10(2): 123–129.

14. Hern DL and Hubbell JA. Incorporation of adhesion peptides into nonadhesive hydrogels useful for tissue resurfacing. *J Biomed Mater Res* 1998; 39: 266–276.

15. Cavalcanti-Adam EA, Micoulet A, Blummel J, et al. Lateral spacing of integrin ligands influence cell spreading and focal adhesion assembly. *Eur J Cell Biol* 2006; 85: 219–224.

16. Gelain F, Bottai D, Vescovi A, et al. Designer self-assembling peptide nanofiber scaffolds for adult mouse neural stem cell 3-dimensional culture. *PLoS One* 2006; 1: e119 (11 pp.).

17. Kumada Y and Zhang S. Significant type I and type III collagen production from human periodontal ligament fibroblasts in 3D peptide scaffolds without extra growth factors. *PLoS One* 2010; 4: e10305 (7 pp.).

18. Banwell EF, Abelardo ES, Adams DJ, et al. Rational design and application of responsive alpha-helical peptide hydrogels. *Nat Mater* 2009; 8(7): 596–600.

19. Pires MM, Przybyla DE and Chmielewski J. A metal-collagen peptide framework for three-dimensional cell culture. *Angew Chem Int Ed Engl* 2009; 48(42): 7813–7817.

20. Berns EJ, Sur S and Pan L. Aligned neurite outgrowth and direct cell migration in self-assembled monodomain gels. *Biomaterials* 2014; 35: 185–195.

21. Silva GA, Czeisler C, Niece KL, et al. Selective differentiation of neural progenitor cells by high-epitope density nanofibers. *Science* 2004; 303: 1352–1355.

22. Guler MO, Hsu L, Soukasene S, et al. Presentation of RGD epitopes on self-assembled nanofibers of branched peptide amphiphiles. *Biomacromolecules* 2006; 7: 1855–1863.

23. Haines-Butterick L, Rajagopal K, Branco M, et al. Controlling hydrogelation kinetics by peptide design for three-dimensional encapsulation and injectable delivery of cells. *Proc Natl Acad Sci USA* 2007; 104: 7791–7796.

24. Jung JP, Moyano JV and Collier JH. Multifactorial optimization of endothelial cell growth using modular synthetic extracellular matrices. *Integr Biol* 2011; 3: 85–196.

25. Zhou M, Smith AM, Das AK, et al. Self-assembled peptide-based hydrogels as scaffolds for anchorage-dependent cells. *Biomaterials* 2009; 30: 2523–2530.

26. Kurkinen M, Isemura M and Yamane I. Sequential appearance of fibronectin and collagen in experimental granulation tissue. *Lab Invest* 1980; 43: 47–51.

27. Welch MP, Odland GF and Clark RAF. Temporal relationships between F-actin bundle formation, fibronectin and collagen assembly, fibronectin receptor expression and wound contraction. *J Cell Biol* 1990; 110: 133–146.

28. Potts JR and Campbell ID. Fibronectin structure and assembly. *Curr Opin Cell Biol* 1994; 6: 648–655.

29. Clark RAF, Nielsen LD, Welch MP, et al. Collagen matrices attenuate the collagen-synthetic response of cultured fibroblasts to TGF-β. *J Cell Sci* 1995; 108: 1251–1261.